DFT studies on electronic and structure properties of $PbSe_{1-x}S_x$ alloys using VCA and EBS

Montiel-Perales S.J.[1], Guarneros-Aguilar C. [2], Boujnah, M[3], Caballero-Briones F.[1,*]

[1] *Instituto Politécnico Nacional, Materiales y Tecnologías para Energía, Salud y Medio Ambiente (GESMAT), CICATA Altamira. Km 14.5 Carr. Tampico- Puerto Industrial Altamira.89600, Altamira, México.*

[2] *CONACYT- Instituto Politécnico Nacional, Materiales y Tecnologías para Energía, Salud y Medio Ambiente (GESMAT), CICATA Altamira. Km 14.5 Carr. Tampico- Puerto Industrial Altamira.89600, Altamira, México.*

[3]*CINVESTAV-Querétaro. Libramiento Norponiente 2000, Fracc. Real de Juriquilla, 76230, Querétaro, Mexico*

*Corresponding author e-mail: fcaballero@ipn.mx

Abstract. In this study, density functional theory has been used to investigate the structural and electronic properties of lead selenide (PbSe) and lead sulfide (PbS) semiconductors and their alloys $PbSe_{1-x}S_x$ using the virtual crystal approximation (VCA) and random structure (RS) generations. The generalized gradient approximation (GGA) has been used to obtain lattice parameters which are compared with theory and experimental results. The generalized gradient approximation (MGGA) of TB09LDA has been used to calculate the electronic bands, for different sulfur compositions ($0 \leq x \leq 1$, $\Delta x = 0.1$). It has been observed that the transition from the valence band to the conduction band takes place at the L point, which agrees with previous theoretical investigations. It has been observed that both the bandgap and lattice parameters of the alloys obey Vegard's law. Effective band diagrams obtained from the unfolding of supercell band diagrams, reported for the first time for this system, show that the impacts of alloy disorder are low in the vicinity of the L point, indicating that the alloy composition do not appear to influence the transport phenomena. This work shows the suitability of the

VCA approximation and the band unfolding method, to deal and describe the composition-dependent properties of the $PbSe_{1-x}S_x$ pseudo binary alloys.

Keywords: lead chalcogenides, ternary alloys, DFT, VCA, EBS

1. Introduction

Group IV-VI semiconducting materials and their heterostructures are well-known for their ability to form ternary and quaternary compounds with direct electronic transitions in nearly their entire composition range [1], with high absorption coefficients, which makes them suitable for the fabrication of photovoltaic and photodetector devices [2]. In addition, the production of these alloys frequently results in a decrease in the thermal conductivities of the materials, which has prompted interest in their possible application as thermoelectric materials [3–5]. Within this group of semiconductors, lead chalcogenides stand out: lead sulfide (PbS), lead selenide (PbSe), and lead telluride (PbTe), the latter being the most widely studied and employed [6], however, telluride is a very scarce material in the Earth's crust [7] and its use in other areas has increased its demand which has caused its price to rise, so it is necessary to find telluride-free alternatives. On the other hand PbSe and PbS are both materials with a narrow bandgap and a direct transition at the L-point of the Brillouin zone that are capable of generating solid alloys throughout the whole composition range [8,9], i.e. $PbSe_{1-x}Se_x$.

Several groups have prepared these alloys in film and bulk form [1,10–19], but no extensive studies on the effect of composition on the band structure have yet been conducted, thus additional experimental and first-principles research is required. In this work seeking to increase the understanding of this system, the results of first-principles calculations of the binary compounds and their $PbSe_{1-x}S_x$ alloys by two approaches are reported, using

Density Functional Theory with the random structure (RS) generation, and the virtual crystal approach (VSA).

2. Computational methods

All calculations were performed using Quantum ATK [20] within the framework of density functional theory (DFT). Electron-ion interactions are expressed using pseudopotentials of the Fritz Haber Institute (FHI) type, and single-electron Kohn-Sham functions are expanded in a linear combination of numerical real-space atomic orbitals (LCAO) as double zeta polarized basis sets. The meta-GGA method, established by the TB09 function, was used to deal with the exchange-correlation interaction. The density grid cutoff was set to 150 Hartree, and the Fermi-Dirac method with a broadening of 86 meV was chosen as the occupancy method. The sampling plan of the k-point grid by Monkhorst-Pack was set to 9x9x9 for the few-atom cells and for the 6x6x6 supercells. In the PulayMixer algorithm, the energy tolerance for the self-consistent field iteration was set to 0.0001 Hartree. For the systems calculated through the virtual crystal approximation, the LBFGS optimizing method was chosen to improve the geometry. The convergence criteria were a force error tolerance of 0.05 eV/Å, a strain error tolerance of 0.1 GPa and a maximum step size of 0.2 Å. The number of electrons, considered as valence electrons were 4 for Pb, $6s^2 6p^2$, 6 for Se $4s^2 4p^4$ and 6 for S $3s^2 3p^4$.

Building an accurate model is the most crucial aspect in simulating disordered solid solutions. Although powerful ab initio band structure approaches exist for handling pure transitively symmetric systems, they are typically not immediately relevant to systems containing random substitutions or disordered alloys. There are numerous accurate

approximation approaches for managing disorder in randomly substituted systems and alloys. In this work we compare the results obtained for band unfolding for random alloys against those obtained by the virtual crystal approximation.

2.1 Random alloys

A supercell containing a significant number of atoms was studied to produce random alloys. In this example, a 3x3x3 repetition of the PbSe FCC unit cell, which contains 54 atoms, 27 lead atoms and 27 selenium atoms was examined. The whole series of $PbSe_{1-x}S_x$ compositions was investigated. The alloys were depicted by starting with a matrix of lead selenide and randomly substituting a proportion of selenium atoms with sulfur atoms to resemble the composition under study. To examine the random influence of the alloys, the operation was done ten times for each composition, and in each case the positions of the selenium atoms to be substituted were randomly selected. The band structure of the supercell, which consists of over 850 electronic bands, can be "unfolded" to contain only bands from the primitive cell. A spectral weight is computed during the unfolding process $\left|\left\langle e^{i\boldsymbol{k}\cdot\boldsymbol{r}}\middle|\psi_j, K\right\rangle\right|$, where $\left|\psi_j, K\right\rangle$ is an eigenstate of the supercell at the K-point. If the supercell is merely a replica of a single unit cell, such as a PbSe supercell, the spectral weights will be either 0 or 1, and band unfolding can be accomplished explicitly. The band weights of disordered alloys, such as $PbSe_{1-x}S_x$, can be any real integer between 0 and 1.

2.2 Virtual Crystal Approximation

The virtual crystal approach (VCA) is a different method for simulating a random alloy. In a VCA simulation of $PbSe_{1-x}S_x$, a new virtual atom is produced that is a mixture of Se and S with the proper weights to obtain the

desired composition. Calculations such as lattice constants or band structures can then be done on a primitive cell containing only two atoms: the conventional Pb atom and the virtual Se-S atom. VCA simulations are far less computationally intensive than EBS calculations since supercells are not required. Unlike the EBS method, VCA simulations do not capture any disorder effects.

3. Results and discussion

3.1 Lattice parameters

The structural characteristics of $PbSe_{1-x}S_x$ alloys were determined using an energy minimization approach. The computed equilibrium lattice constant for binary compounds and corresponding ternary alloys is described in Table 1 along with experimental and theoretical data from the literature. The results show a better concordance of the calculated lattice parameter from this work, with the experimental results, showing the suitability of the VCA approximation for this system. The theoretical results found independently by the groups of Labidi [21] and Boukhris [18] in the framework of specials quasirandom structures (SQS) overestimate the lattice parameters of the system, probably because the size of the supercell chosen was too small, as they only examined 8-atoms systems.

Table 1. Lattice parameters for PbSe and PbS and their alloys $PbSe_{1-x}S_x$ obtained experimentally and by DFT calculations.

x	This work	Expt	Other theoretical approaches			
	VCA		ForceField	x	SQS	SQS
0	6.124	6.13[a,e,f]	6.085[d]	0	6.224[b]	6.210[c]
0.1	6.099	6.10[a] 6.11[e]	6.071[d]			
0.2	6.080	6.09[a] 6.10[e] 6.08[f]	6.058[d]	0.25	6.174[b]	6.073[c]
0.3	6.059	6.06[a] 6.07[e]	6.044[d]			
0.4	6.038	6.03[a] 6.05[e]	6.031[d]			
0.5	6.017	5.99[a] 6.03[e]	6.015[d]		6.125[b]	6.128[c]
0.6	5.990	6.0[e]	6.001[d]			
0.7	5.966	5.97[a] 5.99[e]	5.986[d]	0.75	6.071[b]	6.179[c]
0.8	5.940	5.95[a] 5.98[e]	5.970[d]			
0.9	5.913	5.96[e]	5.954[d]			
1	5.882	5.93[a] 5.94[e]	5.937[d]	1	6.011[b]	6.010[c]

a Ref [22]

b Ref [21]

c Ref [18]

d Calculated with force field from Ref [23]

e Ref [24]

f Ref [4]

The lattice parameter calculated in this work for the $PbSe_{1-x}S_x$ alloys fulfil the Vegard's law as shown in Figure 1, with the lattice constant value reducing as x increases because of the progressive substitution of Se by S atoms with smaller ionic radius in the alloy. Our calculated lattice parameter values are in great accordance with experimental data when $0 \leq x \leq 0.7$ and then for the S-rich compositions our calculations underestimated the lattice parameter, as shown in Figure 1.

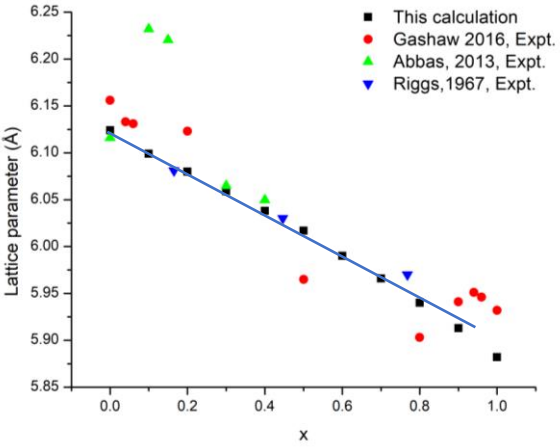

Figure 1. Lattice parameter as a function of the x-fraction in the $PbSe_{1-x}S_x$ alloys, from calculated (this work) and experimental data. Straight line in the calculated data is a guide for the eye.

3.2 Electronic Structure

The electrical nature of a material can be seen through electronic band structure. In materials, energy bands are formed by many closely spaced energy levels. These energy bands are caused by electron wave diffraction within periodic crystalline materials. The energy difference between the valence and conduction bands is known as the band gap, and in this region the existence of electron states is not allowed. The band structure of binary PbS, PbSe compounds, and their ternary alloys, $PbSe_{1-x}S_x$, in rock salt phase is computed using the Meta-GGA. This functional include the local density ρ(r) and the gradient of the density ∇p(r) but also the kinetic-energy density τ(r). Tran and Blaha demonstrated in 2009 [25] that accurate band gaps may be produced for a wide range of materials. The exchange potential is given in their formulation by:

$$v_x^{TB}(r) = cv_x^{BR}(r) + \frac{3c-2}{\pi}\sqrt{\frac{4\tau(r)}{6\rho(r)}} \qquad (1)$$

Here $\tau(r) = \frac{1}{2}\sum_{i=1}^{N} |\nabla\psi_i(r)|^2$ is the kinetic-energy density, ψ_i (r) is the i-th Kohn-Sham orbital, and $v_x^{BR}(r)$ is the Becke-Roussel exchange potential [26].

In MGGA, the functional parameter TB09 c which defines "the exact exchange quantity" can be self-consistently determined by the electron density, or it can be considered as a tuning parameter that can be used to adjust the band gap. In our calculations, the values c = 1.071 and 0.9985 were found to provide optimal gap values for PbSe and PbS respectively. As the accurate c value to optimize the band gap for the intermediate compositions cannot be predicted, the simplest solution to calculated Eg in the 0<x<1 range is to simply interpolate between the c values for PbS and PbSe.

Although TB09 reproduces band gaps at the experimental geometry [27] with remarkable accuracy, it cannot determine the equilibrium lattice constant. For this reason, the lattice constant for the alloys was obtained as an average from the literature values and the VCA results from the previous section [24], and more precisely, a linear fit was made and the following function was used to assign the value of the lattice parameter to each composition.

$$a = 6.12818 - 0.19691 * x \quad (2)$$

Table 2 compares the MGGA band gaps estimated using random structures and VCA for binary compounds and their ternary alloys to other theoretical calculations and practical data from the scientific literature.

Table 2. Forbidden bandgaps for PbSe and PbS and their alloys $PbSe_{1-x}S_x$ obtained experimentally and by DFT calculations.

	This work		**Experimental**	**Other calculations**	**x**
PbSe	0.27[a]	0.278[b]	0.296[c], 0.29[d], 0.37[e]	0.318[g], 0.24[h], 0.43[i] , 0.44[j]	0
$PbSe_{0.9}S_{0.1}$	0.279[a]	0.299[b]	0.356[c], 0.33[f]		
$PbSe_{0.8}S_{0.2}$	0.26[a]	0.309[b]	0.31[d], 0.46[e]	0.365[g], 0.1[h], 0.329[i], 0.331[j]	0.25
$PbSe_{0.7}S_{0.3}$	0.278[a]	0.336[b]	0.338[c]		
$PbSe_{0.6}S_{0.4}$	0.297[a]	0.331[b]	0.368[c], 0.34[d], 0.5[e]		
$PbSe_{0.5}S_{0.5}$	0.321[a]	0.32[b]	0.33[e], 0.363[f]	0.4[g], 0.13[h], 0.34[i], 0.38j	0.5
$PbSe_{0.4}S_{0.6}$	0.32[a]	0.373[b]	0.37[d], 0.37[e],		
$PbSe_{0.3}S_{0.7}$	0.353[a]	0.381[b]		0.2[h], 0.427[i], 0.27[j]	0.75

$PbSe_{0.2}S_{0.8}$	0.381[a]	0.399[b]	0.39[d], 0.39[e], 0.393[f]		
$PbSe_{0.1}S_{0.9}$	0.392[a]	0.405[b]	0.42[f]		
PbS	0.43[a]	0.423[b]	0.42[d], 0.41[e]	0.448[g], 0.3[h], 0.5[i], 0.5[j]	1

a. Calculated with EBS, MGGA

b. Calculated with VCA, MGGA

c. Ref. [8]

d. Ref. [29]

e. Ref. [30]

f. Ref. [15]

g. Ref. [21]

h. Ref. [24]

i. Ref. [23]

j. Ref. [22]

The obtained results for binary PbS and PbSe are consistent with previous experimental data [28]. As demonstrated in the previous section, the Eg of the alloys obey Vegard's law, i.e. there is a linear dependence as a function of concentration x, as found experimentally by Kumar [29] and Mochalov [30] although deviations from the law have been reported by Kumar himself in [31], although these deviations may be due to deviations in the stoichiometry rather than the system itself. On the other hand, the present results differ considerably from previous theoretical results. In Refs [12,18,21,32] a lot of dispersion between the values reported by the authors was observed, as shown in Table 2. The discrepancy in the results can be attributed to a variety of factors, including the selection of inevitable approximations (exchange correlation functional, atom representation, etc.) or to some minor oversights made during a highly sophisticated

computational procedure, as well as to some underlying physical effects (the effect of atom arrangement, insufficient lattice relaxation).

3.2.1 Effective Band Structure

Figure 2 illustrates the band structure along the high symmetry k-points of PbS, PbSe, and their ternary alloys $PbSe_{1-x}S_x$ for various S-concentrations. For each S concentration, the band structure is computed at the equilibrium configuration (rocksalt) using the above-defined lattice constant. The p-states of chalcogen atoms (S, Se) contribute the most to the band just below the Fermi level (VB), while Pb p-electrons predominate in the band just above the Fermi level (CB). The maximum of the valence band (VB) and the minimum of the conduction band (CB) are located above the high symmetry point L, therefore they are direct transition materials.

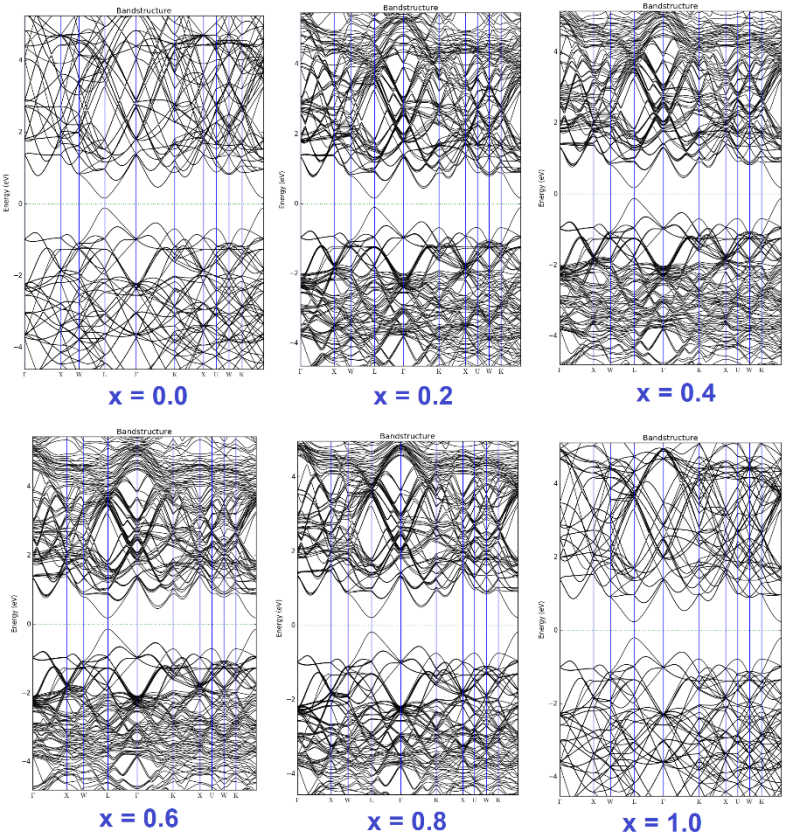

Figure 2. Band structure of a 3x3x3 supercell of the $PbSe_{1-x}S_x$ alloys calculated by MGGA.

Although it is possible to obtain the E versus k diagram straight from a supercell, its interpretation is typically not viable due to the complexity and number of bands involved, as derived from the inspection of Figure 3b. For a better visualization, it is desirable to see these band diagrams within a primitive cell, and the technique known as 'band unfolding' makes this

possible. There are approximately 850 bands per system in the systems studied here, as shown in Figure 3b, therefore they must be "unfolded" to contain only bands from the primitive cell as depicted in Figure 3c; the method is extensively described elsewhere [33–35].

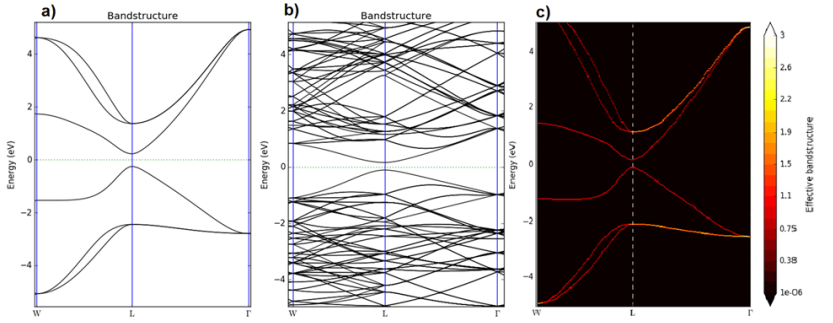

Figure 3. (a) Standard band structure of PbSe (2-atom primitive cell, plotted in primitive Brillouin zone). (b) Supercell band structure (54-atom supercell PbSe, plotted in the same primitive Brillouin zone) and (c) EBS (unfolded from 54-atom supercell for PbSe into the same primitive Brillouin zone). (a) (b) and (c) are plotted along the same X-L direction in the primitive Brillouin zone.

Briefly, we employ a method that develops an "effective band structure" (EBS) for disordered alloys in the Brillouin zone of their parent components. The proposed method, however, is based on a fully polymorphous supercell (SC) description of the alloy, as opposed to models that ignore variations from the start [36–38]. The substitutionally disordered alloy is initially described using large SCs, including potentially tens or hundreds of atoms

with randomly (or correlated) distributed site occupancy, permitting polymorphous forms.

First, the alloy eigenstates are obtained by diagonalizing the SC Hamiltonian. $\{\langle\varepsilon_i|\Psi_i\rangle\}$ then, one determines how much of the Bloch character k remains in the alloy states. The selection of the Brillouin zone in which k is contained can be entirely independent of the selection and symmetry of the SC. Consequently, in accordance with the criterion that the accurate ensemble average of the charge density in a substitutional alloy has the periodicity of the underlying lattice, we end up with the symmetry of the components but begin with a lower symmetry of the SC. Unfolding the SC results into the selected Brillouin zone results in a dispersion relationship, which depicts the consequences of the existence of a multitude of local environments via broadening and dispersion of the EBS's effective $E(\vec{k})$ relation [34].

To the best of our knowledge, this kind of alloys' band diagrams have never been published. Figures 4(a-d) depict the effective band diagrams for x = 0.2, 0.4, 0.6, and 0.8. As it is well known that the minimum of the conduction band and the maximum of the valence band are positioned above the L point of the Brillouin zone for both pure PbSe and PbS, the band dispersion is essentially equal for the bands close to the Fermi level in both materials.

In the case of alloys, as depicted in Figure 4, the bands of electrons and light holes are highly dispersive and 100 percent coherent around the L point. However, as they move in the Λ (L-Γ) and Q (L-W) directions, they rapidly lose coherence, particularly at the W and Γ points. On the other hand, we can observe that the heavy electron and heavy hole bands are significantly deformed in the (L-) and Q (L-W) directions, although they are well-defined at the L point.

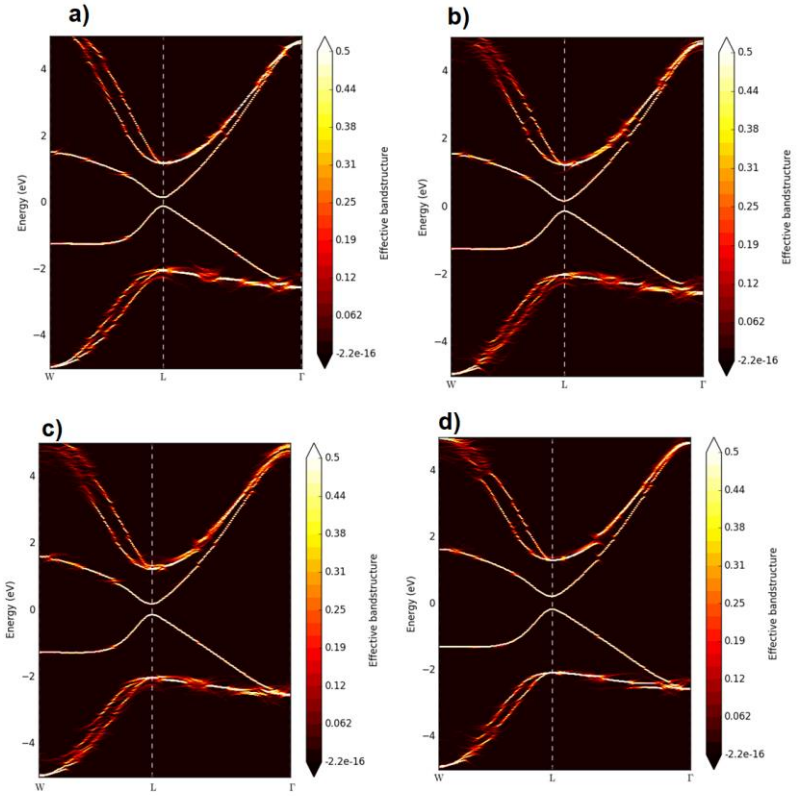

Figure 4. Unfolded band structure of a 3x3x3 supercell of the $PbSe_{1-x}S_x$ alloys (a) x=0.2 (b) x=0.4 (c) x=0.6 (d) x=0.8

The well-defined effective band structure around the L-point can be attributed to the presence of a long wavelength. Long-wavelength electrons cannot "perceive" random local fluctuations. In contrast, in the Λ and Q directions, the wave functions vary on an atomic scale and are affected by the disorder of the local alloy environments.

Since the wave function is entirely specified at the L point, we can assume that Bloch's theorem holds, thus disorder has a negligible impact on the transport properties.

Conclusions

In the present contribution, the effect of the composition of $PbSe_{1-x}S_x$ alloys on their lattice parameter and band diagram was investigated. Lattice parameters calculated using VCA shows the better accordance with experimental data, compared with other reported results. The dispersion of electronic bands was studied using VCA and band splitting to determine the effective bands of random alloys. It was observed that all alloys have the conduction band minima and valence band maxima at the same high symmetry point L. The lattice parameter and forbidden band gap values were found to vary linearly with alloy composition, i.e. they follow the Vegard's law. Based on the effective band diagrams, reported for the first time for this system, it was determined that the impacts of alloy disorder are low in the vicinity of the L point, indicating that the alloy composition do not appear to influence the transport phenomena; nonetheless, additional research is required in this regard.

Acknowledgments

This work has been supported by CONACYT Basic Science Grant CB-2016-286059 and MSc grant, and BEIFI-IPN through the project 20220834. The authors acknowledge Laboratorio Nacional de Supercómputo del Sureste de México (LNS), a member of CONACYT national laboratories, for the computational resources provided through project nº 202201032N.

References

[1] M S Othman, S M Hamad, and H Y Abdullah *J. Kerbala Univ.* 12 221 (2016).

[2] G Bauer and G Springholz *SEMICONDUCTOR MATERIALS | Lead Salts* (ed) R D Guenther, (Oxford : Elsevier) p 385 (2005).

[3] C Gayner, K K Kar, and W Kim *Mater. Today Energy* 9 359 (2018).

[4] J Androulakis, I Todorov, J He, D-Y Chung, V Dravid, and M Kanatzidis *J. Am. Chem. Soc.* 133 10920 (2011).

[5] A A Khan, I Khan, I Ahmad, and Z Ali *Mater. Sci. Semicond. Process.* 48 85 (2016).

[6] Q Zhang, F Cao, W Liu, K Lukas, B Yu, S Chen, C Opeil, D Broido, G Chen, and Z Ren *J. Am. Chem. Soc.* 134 10031 (2012).

[7] J Sun, X Su, Y Yan, W Liu, G Tan, and X Tang *ACS Appl. Energy Mater.* 3 2 (2019).

[8] W W Scanlon *J. Phys. Chem. Solids* 8 423 (1959).

[9] J W Earley *Am. Mineral. J. Earth Planet. Mater.* 35 337 (1950).

[10] N K Abbas, E M Al-Fawade, and S J Alatya *J. Mater. Sci. Eng. A* 3 82 (2013).

[11] T Djaafri *PhD Thesis* (université ibn khaldoun-tiaret) (2017).

[12] S Kacimi, A Zaoui, B Abbar, and B Bouhafs *J. Alloys Compd.* 462 135 (2008).

[13] E M Nasir, N K Abas, and S J Alatya *Int. J. Thin Film Sci. Technol.* 2 9 (2013).

[14] O Maksimov, P Su, P Bhattacharya, K E Stoll, K Wada, L C Kimerling, A Agarwal, and H B Bhandari *Thin Solid Films* 731 138749 (2021).

[15] B A Riggs *J Electrochem Soc* 114 708 (1967).

[16] Y S Sarma, H N Acharya, and N K Misra *Thin Solid Films* 90 L43 (1982).

[17] Y S Sarma, H N Acharya, and N K Misra *Infrared Phys.* 24 425 (1984).

[18] N Boukhris, H Meradji, S Ghemid, S Drablia, and F E H Hassan *Phys. Scr.* 83 065701 (2011).

[19] F G Hone, F K Ampong, R K Nkum, and F Boakye *J. Mater. Sci. Mater. Electron.* 28 2893 (2017).

[20] S Smidstrup, T Markussen, P Vancraeyveld, J Wellendorff, J Schneider, T Gunst, B Verstichel, D Stradi, P A Khomyakov, U G Vej-Hansen, and others *J. Phys. Condens. Matter* 32 015901 (2019).

[21] M Labidi, H Meradji, S Ghemid, S Labidi, and F El Haj Hassan *Mod. Phys. Lett. B* 25 473 (2011).

[22] J L Wang, H Wang, G J Snyder, X Zhang, Z H Ni, and Y F Chen *J. Phys. Appl. Phys.* 46 405301 (2013).

[23] Z Fan, R S Koster, S Wang, C Fang, A O Yalcin, F D Tichelaar, H W Zandbergen, M A Van Huis, and T J Vlugt *J. Chem. Phys.* 141 244503 (2014).

[24] R Neuelmann, A Marino, and K Reichelt *J. Cryst. Growth* 64 609 (1983).

[25] F Tran and P Blaha *Phys. Rev. Lett.* 102 226401 (2009).

[26] A D Becke and M R Roussel *Phys. Rev. A* 39 3761 (1989).

[27] K Sakata, B Magyari-Köpe, S Gupta, Y Nishi, A Blom, and P Deák *Comput. Mater. Sci.* 112 263 (2016).

[28] M Cardona and D L Greenaway *Phys Rev* 133 A1685 (1964).

[29] S Kumar, M M Khan, S A Khan, and M Husain *Opt. Mater.* 25 25 (2004).

[30] L Mochalov, A Logunov, M Kudryashov, Y Kudryashova, M Vshivtsev, and V Malyshev *Opt. Mater. Express* 12 1741 (2022).

[31] R Kumar, G Jain, R Saini, and P Agarwal *Chalcogenide Lett.* 7 233 (2010).

[32] G Murtaza, R Khenata, N Hassan, S Naeem, M Khalid, S B Omran, and others *Comput. Mater. Sci.* 83 496 (2014).

[33] V Popescu and A Zunger *Phys. Rev. Lett.* 104 236403 (2010).

[34] V Popescu and A Zunger *Phys. Rev. B* 85 085201 (2012).

[35] M W Haverkort, I S Elfimov, and G A Sawatzky *ArXiv Prepr. ArXiv11094036* (2011).

[36] J Faulkner and G Stocks *Phys. Rev. B* 21 3222 (1980).

[37] A-B Chen and A Sher *Semiconductor alloys: physics and materials engineering* (Springer Science & Business Media) (1995).

[38] N J Ramer and A M Rappe *Phys. Rev. B* 62 R743 (2000).